Journal of Colloid and Interface Science 383 (2012) 82–88

Contents lists available at SciVerse ScienceDirect

Journal of Colloid and Interface Science

www.elsevier.com/locate/jcis

Synchronous One-Pot (**SOP**) synthesis of hybrid structures: Metal nanoparticles in self-assemblies of amphiphilic calix[6]biscrowns

Qing Liang, Changxi Li, Guosong Chen *, Ming Jiang *

State Key Laboratory of Molecular Engineering of Polymers, Department of Macromolecular Science, Fudan University, 220 Handan Rd., Shanghai 200433, China

ARTICLE INFO

Article history:
Received 31 March 2012
Accepted 5 June 2012
Available online 23 June 2012

Keywords:
Calixarene
Gold nanoparticle
Self-assembly
Catalysis
Hydrogenation

ABSTRACT

In this paper, we present a novel strategy, named Synchronous One-Pot (**SOP**) synthesis, to prepare gold nanoparticles (AuNPs) with a diameter of 2 nm incorporated in self-assembled organic spheres with a diameter around 60 nm (denoted as **NPAs**). Merits of this method include: (1) self-assembly of the organic component (calix[6]biscrown TAC) into spheres and the reduction of chloroauric acid ($HAuCl_4$) take place simultaneously; (2) preparation combining UV irradiation and formaldehyde addition reduces the size and homogenizes the distribution of the resultant AuNPs within the TAC spheres. (3) Obtained material **NPA** gives attractive catalytic property to hydrogenation reaction.

1. Introduction

Metal nanoparticles (NPs) attract great interest because of their varieties of outstanding properties [1]. Thinking further from the relevant achievements in literature, self-assembly of NPs into well-defined supra-structures (**NPA**s), is imperative and challenging to further explore their fascinating properties [2]. Briefly, **NPA** is made of metal NP itself and organic matrix, the latter is usually called nanocarrier. Generally, the NPs and nanocarriers can be prepared concurrently or sequentially [3]. Many sequential preparative methods of **NPA**s have been reported. Here, the precursors of NPs, for example, chloroauric acid for AuNPs, may be introduced directly into the preformed nanocarrier, and then reduction and immobilization take place. Many different carrier systems have been utilized by this two-step method in one-pot, including dendrimers [4], microgels [5], etc. However, unreacted chemicals from the first step may disturb the second step and thus affect the desired structures and properties of the final **NPA**s. The concurrent strategy is preferable as it could avoid tedious purification and extra chemicals. As an example, recently Rosi et al. reported simultaneous self-assembly of synthetic peptides and reduction of chloroauric acid, resulting in AuNPs in the helix structure of peptides [6]. However, until now, **NPA** structures prepared by such simple method are still rare in literature.

Our group has studied continuously on self-assembly of amphiphilic calixarenes bearing two crown ether loops, named calix[6]biscrowns, which gave out uniform assembled structures in media with certain polarity [7]. The self-assembly process is fast, versatile, and controllable. Furthermore, the primary amine groups, which can be easily introduced to the calixarene, could serve as a good reducing reagent and stabilizer for the following formation of metal NPs. This inspires us to explore a real one-pot and concerted strategy for **NPA** preparation, in which the assembly formation of calixarene and metal ion reduction take place simultaneously. It is worth to mention that, although derivatives of calixarenes are routine ligands of various metal NPs [8], reports about the self-assembled calixarenes as nanocarriers for NPs are very limited. Recently, via a two-step method, we successfully prepared and immobilized AuNPs onto the surface of nanotubes made of our calix[6]biscrowns, assisted by the common reducing agent $NaBH_4$ [9]. Herein, we report a new strategy that the self-assembly of calix[6]biscrowns is performed simultaneously with photochemical reduction of chloroauric acid, which is named Synchronous One-Pot (**SOP**) synthesis. UV light was selected as a versatile and clean energy source [10]. In the presence of formaldehyde, the AuNPs obtained in **NPA** were as small as 2 nm in diameter. Furthermore, the catalytic properties of **NPA**s in hydrogenation of α,β-unsaturated aldehydes were investigated.

2. Experimental section

2.1. Materials

All materials and reagents were obtained from commercial suppliers for direct use. Calix[6]biscrown **TAC** was synthesized according to our reported procedure [7].

* Corresponding authors. Fax: +86 21 65643919.
E-mail addresses: guosong@fudan.edu.cn (G. Chen), mjiang@fudan.edu.cn (M. Jiang).

0021-9797/$ - see front matter © 2012 Elsevier Inc. All rights reserved.
http://dx.doi.org/10.1016/j.jcis.2012.06.006

2.2. Measurements

TEM was performed on a Philips CM 120 electron microscope. For sample preparation, a small droplet of the solution was deposited onto a carbon-coated copper grid and then dried at room temperature. HR-TEM was performed on a JEM-2100F electron microscope (Accelerating Voltage: 200 kV, Point Resolution: 0.19 nm). TEM–EDX was adopted on a Philips CM 120 electron microscope with a QUANTAX 400 energy dispersive X-ray spectrum as an accessory. ^{13}C NMR was carried out on a Bruker (500 MHz) NMR instrument, using CD_3OD as solvent. XPS experiments were carried out on a RBD upgraded PHI-5000C ESCA system (Perkin Elmer) with Mg Kα irradiation ($h\nu$ = 1253.6 eV) or Al Kα irradiation ($h\nu$ = 1486.6 eV).

2.3. Preparation of *NPA-10*

The hybrid nanoparticles **NPA-10** was named as the average diameter of AuNPs was about 10 nm. The preparation of **NPA-10** was as follows: the aqueous solution of $HAuCl_4$ (1 mL, 0.5 mg mL^{-1}, 1.48 × 10^{-3} mmol) was dropwisely added into 1 mL ethanol solution of **TAC** (1 mg mL^{-1}, 0.7 × 10^{-3} mmol). Subsequently, the solution was irradiated with UV light (365 nm, 90 W) with continuously stirring within 1 h, and the hybrid nanoparticles **NPA-10** formed in this mixed solution of water/ethanol (v:v = 1:1).

2.4. Preparation of *NPA-2*

The **NPA-2** was named as the average diameter of AuNPs was about 2 nm. The preparation of **NPA-2** was as follows: the aqueous solution of 1 mL $HAuCl_4$ (0.5 mg mL^{-1}, 1.48 × 10^{-3} mmol) containing 200 μL formaldehyde (37–40% aqueous solution) was added into 1 mL **TAC** solution in ethanol (1 mg mL^{-1}, 0.7 × 10^{-3} mmol). After stirring under UV light irradiation for 1 h, the **NPA-2** with uniform AuNPs with a diameter of 2 nm were prepared.

2.5. The selective hydrogenation reaction using *NPA*s as catalyst

The liquid phase hydrogenation of crotonaldehyde (CRAL) setup described in literature [11] was employed. The hydrogenation was carried out in a 100 mL stainless steel autoclave in which 2.5 mg of the catalyst (**NPA**, containing variable mount of AuNPs), 0.1 mL CRAL, and 20 mL water were loaded. The reaction vessel was sealed and purged six times with pure hydrogen. After reaching the required temperature (373 K), the H_2 pressure was raised to 2.0 MPa and stirring (1000 rpm) was commenced. This is taken as the beginning of the reaction. The reaction progress was monitored by analyzing the samples withdrawn from the autoclave at intervals on a gas chromatograph (Finnigan Trace GC Ultra) equipped with XE-60 capillary column (30 m × 0.32 mm) and a flame ionization detector (FID). Catalysis of **NPA** was evaluated in triplicate, and results from replicate runs agreed to within 2%.

3. Results and discussion

3.1. Formation of *NPA*s

Typical preparation of the **NPA**s by **SOP** can be described as follows. After aqueous solution of $HAuCl_4$ (1 mL, 0.5 mg mL^{-1}, 1.48 × 10^{-3} mmol) was dropwisely added into 1 mL ethanol solution of **TAC** (1 mg mL^{-1}, 0.7 × 10^{-3} mmol, Scheme 1), the solution was irradiated with UV light (365 nm, 90 W) with continuously stirring within 1 h. It was observed that the solution color changed from bright yellow to colorless, and then to deep red, indicating the photochemical reduction of Au^{3+} to Au^{+} then Au^0, and the final formation of AuNPs [12]. This result indicated that with UV irradiation, AuNPs were easily generated in situ with the amine groups on **TAC** as a reducing reagent and stabilizer. From TEM (Transmission Electron Microscopy) image (Fig. 1a), AuNPs were found to disperse within the organic spheres ununiformly. For clarity, the obtained **NPA** was named **NPA-10**, as the average diameter of AuNPs was about 10 nm (Fig. 1b).

One of the major goals to prepare the **NPA** structure is to achieve better catalytic properties of AuNPs, which greatly depends on the particle size [13]. Uniform nanoparticles with a small diameter (<3 nm) are desirable to achieve this goal. Formaldehyde was reported as a promoting agent to decrease the size of metal NPs [14], but seldom used in photo reduction chemistry. In current work, aqueous solution of 1 mL $HAuCl_4$ (0.5 mg mL^{-1}, 1.48 × 10^{-3} mmol) containing 200 μL formaldehyde (37–40% aqueous solution) was added into 1 mL **TAC** solution in ethanol (1 mg mL^{-1}, 0.7 × 10^{-3} mmol). After stirring under UV light irradiation for 1 h, as shown in Fig. 2a and b, differing from the previous results without formaldehyde, relatively uniform AuNPs with a peak diameter of 2 nm (**NPA-2**) incorporated in the assembled spheres of **TAC** with a diameter of 60 nm were observed via HR-TEM (high resolution TEM). Meanwhile, magnified TEM images showed a clear organic layer of TAC surrounding AuNPs (Fig. 2d and f). Further amplified HR-TEM image displayed clear polyhedral crystal lattices (Fig. 2c) with a lattice distance of 0.225 nm, which is close to that of the Au (1 1 1) (0.23 nm) of the face centered cubic (fcc). Furthermore, the energy dispersive X-ray spectrum (EDX) clearly showed the characteristic peak of Au (the inset of Fig. 2c). In addition, X-Ray photoelectron spectroscopy (XPS) also confirmed the reduction as the binding energy of Au at 88.6 and 85.0 eV (Fig. 2e). We observed that the absorption peak in UV–vis spectra appeared at 525 nm (Fig. 2e) which corresponded well with the red color of the obtained solution but was not consistent with the observed diameter of AuNPs as small as 2 nm. As shown in more TEM images, AuNPs in the present work with a diameter larger than 5 nm are hard to find (Fig. S1); however, the population of AuNPs larger than 3 nm (Fig. 2b) in diameter seems enough to provide the bands at around 525 nm. Combining these results, it could be concluded that **SOP** synthesis of AuNPs during the self-assembly of amphiphilic calix[6]biscrowns has been achieved under a combination of UV irradiation and formaldehyde addition. Compared to **NPA-10**, AuNPs in **NPA-2** have much narrower size distribution and thus are employed for further study.

In order to explore the **SOP** process in detail, morphology evolution of the self-assembly with reaction time was monitored (Fig. 3). At the beginning of the reaction, the mixed solution changed from bright yellow to colorless within a few minutes, indicating the reduction of Au^{3+} to Au^{+}. The TEM image for the sample obtained after 10 min of UV irradiation only showed some light-gray vesicles, while AuNPs were hardly found (Fig. 3a). The colorless solution was then kept for 20 min under UV light before its color gradually turned to red. The TEM image of the sample at

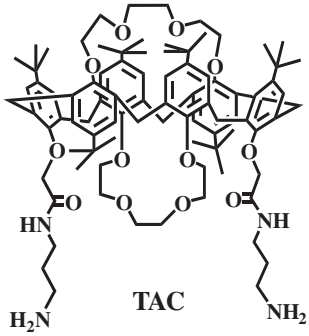

Scheme 1. The structure of amphiphilic calix[6]biscrown **TAC**.

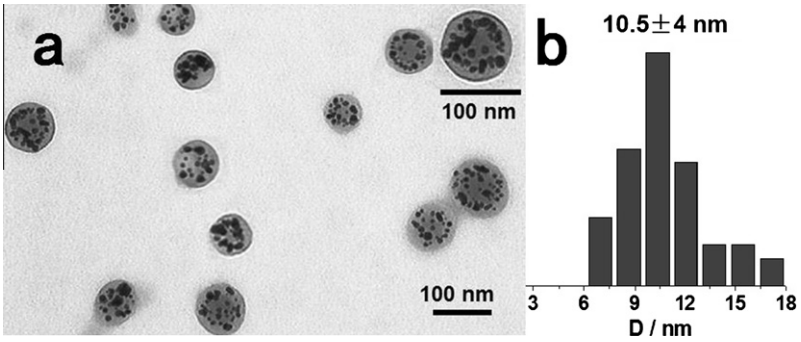

Fig. 1. (a) TEM image of **NPA-10** and (b) size distribution of the AuNPs inside.

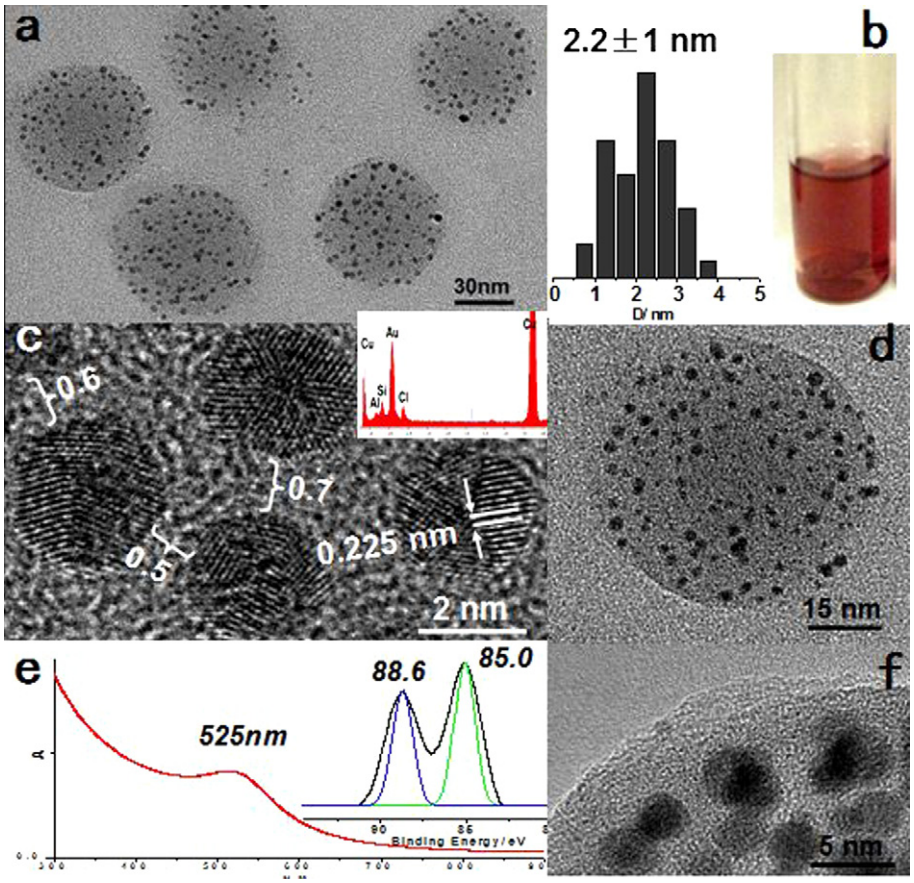

Fig. 2. HR-TEM images (a, c, d, f) show the hybrid nanostructure of **NPA-2**, amplifying sequence: a–d–f–c. The size distribution of AuNPs and the solution picture are shown in (b), as well as the corresponding EDX (inset in c), XPS data (inset in e), and UV–vis spectra (e).

30 min interval showed that the AuNPs appeared and dispersed uniformly in the organic spheres (Fig. 3b). Then, more and more well-dispersed hybrid particles were observed, while the AuNPs inside the spheres were uniform with a diameter around 2 nm (Fig. 3c and d). This process was also monitored by UV–vis spectroscopy (Fig. S2). The characteristic absorption peak of **NPA-2** was found at 530 nm at first, and then a slight blue shift was observed as the reaction proceeded, indicating the gradual size increase in AuNPs in the **NPA**s.

3.2. Influence of $HAuCl_4$ on morphology of *NPA*

We already proved that [7] **TAC** self-assembled into uniform vesicles or nanotubes in water/ethanol depending on the medium polarity. Briefly, **TAC** gave vesicles in water/ethanol (*v*:*v* = 1:3), and nanotubes in water/ethanol 1:1. In the present case, although the mixed solvent of high polarity (water/ethanol 1:1) was used, only spheres instead of tubular structures were observed when aqueous $HAuCl_4$ solution instead of pure water was employed (Fig. 3a). In our very recent research, the presence of amide group in **TAC** had been proved to be a crucial reason for nanotube formation [15]. However, in this case, since the acidity of $HAuCl_4$ is strong enough to protonate the terminal amine in **TAC**, the corresponding $AuCl_4^-$ may surround **TAC** as counterions [16]. This protonation increases the hydrophilicity of the terminal groups, then decreases the molecular curvature of **TAC**, and finally promotes the formation of spheres instead of nanotubes. Another possible reason is that, the nanotube structure requires the hydrophilic end of the

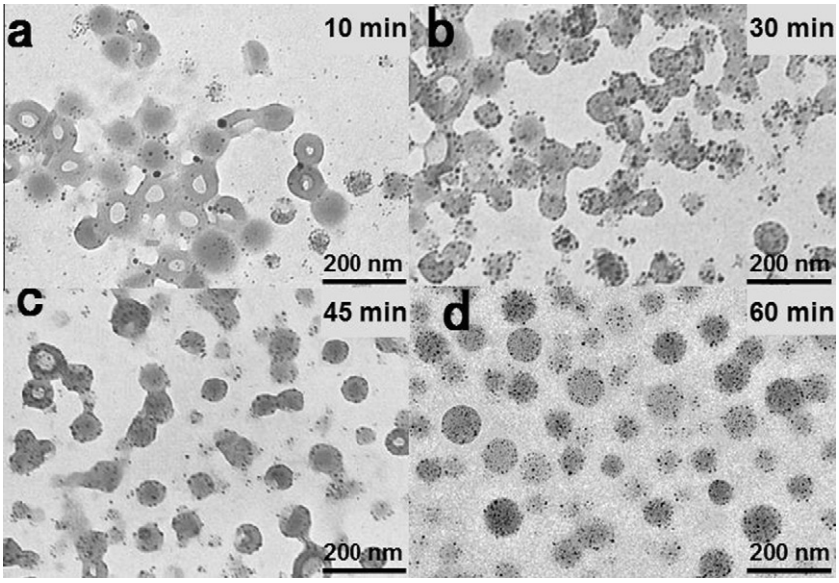

Fig. 3. (a–d) TEM images of the reaction solution taken at different time interval of 10, 30, 45, 60 min.

molecule to be more compact than that in spheres, the electronic repulsion between NH_3^+ ions may also disfavor this trend.

$HAuCl_4$ concentration is another factor to control **NPA**. A series of $HAuCl_4$ solutions in a concentration range from 0.05 to 1.0 mg/mL were employed to prepare **NPA-2**. As the concentration of $AuCl_4^-$ increased, the special surface plasmon peak of AuNPs obtained after 1 h UV irradiation became more and more obvious (Fig. S3). At the relatively low concentration of 0.10 mg/mL of $AuCl_4^-$, the absorption peak appeared at 515 nm. This peak red-shifted to around 525 nm when the concentration increased to 0.50 mg/mL. Then, it shifted further to around 541 nm when the concentration reached 1.0 mg/mL. This trend was explored by TEM too (Fig. S4), where the morphology of the **NPA** changed as the concentration of $AuCl_4^-$ increased. At a low concentration, the amount of $AuCl_4^-$ was not enough to tune the curvature of **TAC**, so the irregular spheres or other morphologies were observed (Fig. S4a). The spherical structure became more and more uniform and well-dispersed as the $AuCl_4^-$ concentration increased.

3.3. Possible role of formaldehyde

As we mentioned, formaldehyde played an important role to form **NPA-2**. After addition of formaldehyde, smaller and more uniform size of AuNPs in **TAC** nanocarrier were observed, so we speculate that the AuNPs are surrounded by a stronger stabilizer rather than the original terminal amine of **TAC**. Herein, the role of formaldehyde was explored by ^{13}C NMR spectrum. After addition of formaldehyde to the solution of **TAC**, a couple of new peaks were observed around 85–95 ppm. So in this mixed solution, amines from **TAC** may attack the carbonyl carbon in formaldehyde to form NH—CH_2—OH as an intermediate moiety, because only the carbon in **TAC** connected to both nitrogen and oxygen could present the signal in this chemical shift range (Fig. 4b). The possible chemical reaction is shown in Fig. S5. A similar phenomenon in NMR spectrum was also observed by Sun et al. [17]. Because of the characteristic sp^3 hybridization of the methylene carbon in NH—CH_2—OH, this N—C—O structure with a bond angle around 109° may serve as a better stabilizer than amine, that is, the N atom and O atom could stabilize AuNPs simultaneously as shown in Fig. 4a and then lead to smaller AuNPs. Moreover, formaldehyde was reported as a reducing agent to increase the number of initial nuclei [18], which could be another possible reason to decrease the size of AuNPs.

This **SOP** method was then expanded to other noble metals. Ag^+ ($AgNO_3$) and Pt^{4+} (H_2PtCl_6) were employed under the similar experimental conditions in the presence of formaldehyde for 1 h reaction. As shown in Fig. 5, **NPA**s of Ag and Pt similar to those of Au were observed. Spheres formed by **TAC** were uniform in diameter as that incorporating AuNPs. TEM–EDX spectra confirmed the existence of Ag (inset of Fig. 5c) and Pt (inset of Fig. 5d). XPS results further revealed the binding energy at 374.4 and 368.8 eV for AgNPs, as well as 75.5 and 71.4 eV for PtNPs (Fig. 5c and d). It is worth to mention that, primary amine is known as a versatile binding reagent to various metal ions, including Ag^+ [19], which may also change the polarity of **TAC** and leads to the formation of spheres instead of nanotubes. Considering the affinity of calixarene to various metal ions [8], this **SOP** method might be a promising and universal one to prepare **NPA**s for many different metal NPs, which might bring interesting catalytic applications.

3.4. The catalytic properties of *NPA*s

To investigate the catalytic properties of the assembled AuNPs (**NPA-10** and **NPA-2**), hydrogenation of a typical α,β-unsatured aldehyde crotonaldehyde (CRAL) was chosen as a model reaction. In principle, CRAL has three hydrogenation products, *i.e.* butanol (BUAL), crotyl alcohol (CROL), and butanol (BUOL) (Fig. 6c). The hydrogenation selectivity of C=C bond and C=O bond had attracted great interest as a classical reaction for selectivity [20]. In our study, the catalytic reaction of CRAL was performed at 373 K under 2 MPa.

H_2 atmosphere in pure water with a catalytic amount of **NPA**s, which were pretreated by dialysis against water in order to remove extra alcohol and formaldehyde. Water was chosen as reaction medium for reducing pollution, just as in our previous study [9]. As shown in Fig. 6a, the reaction led to CRAL decrease obviously while BUAL increased sharply. The other two products CROL and BUOL were in rather low conversions during the reaction. More importantly, **NPA-2** showed a high selectivity on C=C bond as the production of BUAL (79.42%) was much higher than CROL (9.92%) at a moderate CRAL conversion (48.4%). (Table S1). According to

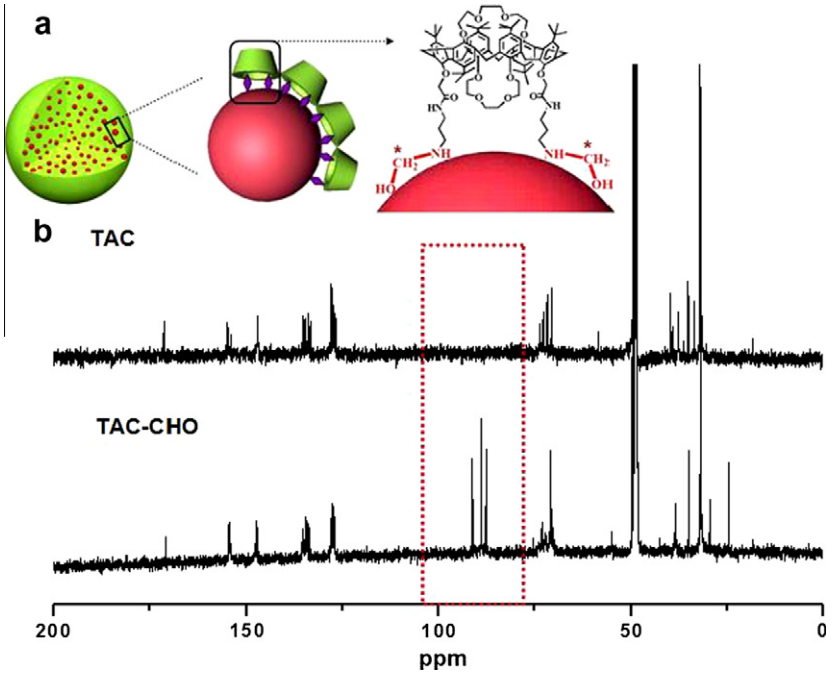

Fig. 4. Scheme (a) of **NPA-2** with a proposed stabilizer formed by **TAC** with formaldehyde; (b) ^{13}C NMR spectra of **TAC** in the absence (**TAC**) and presence (**TAC**-CHO) of formaldehyde in CD_3OD.

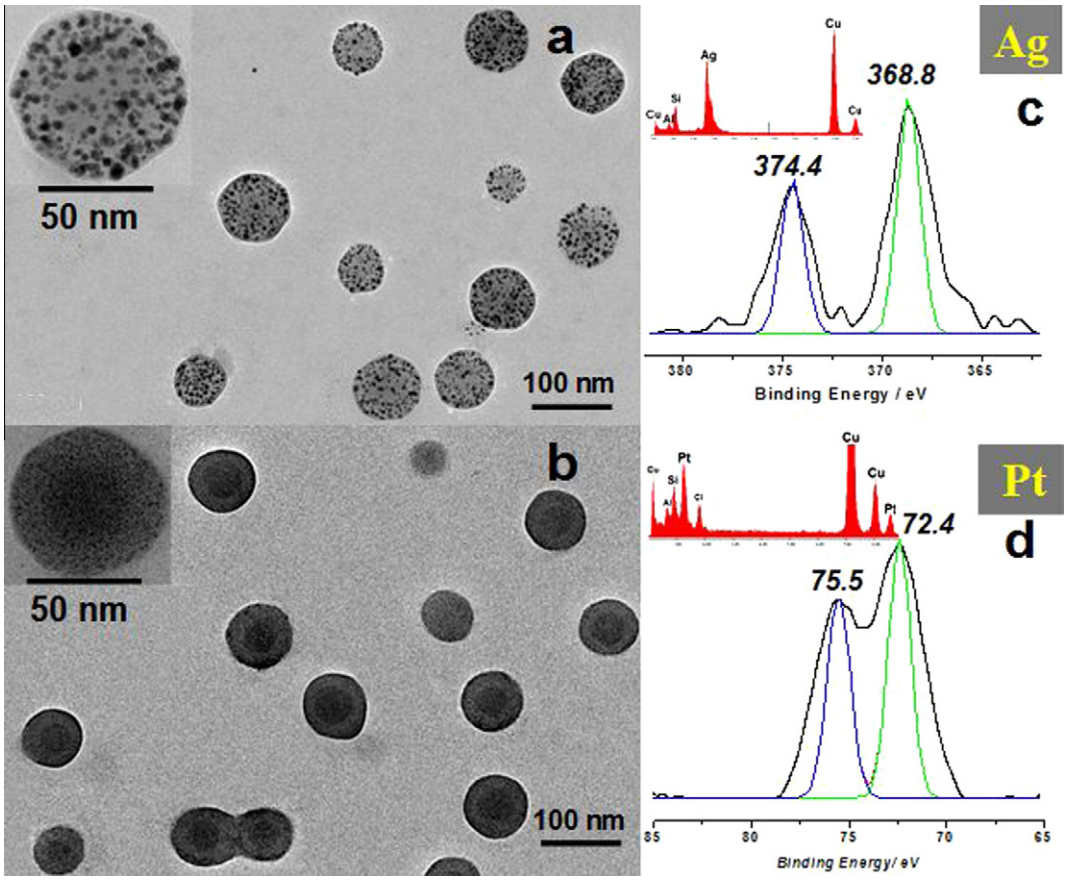

Fig. 5. TEM images, XPS and EDX results of assembled AgNPs (a and c) and PtNPs (b and d).

the literature [21], this phenomenon can be explained by the more negative reaction enthalpy of C=C bond (-16.9 kcal mol^{-1}) than that of C=O (-7.3 kcal mol^{-1}), favoring the C=C hydrogenation thermodynamically. Besides, C=C bond also has a higher activity than C=O for kinetic reasons. Compared to our previous research results about AuNPs with 8 nm diameter in self-assembled TAC

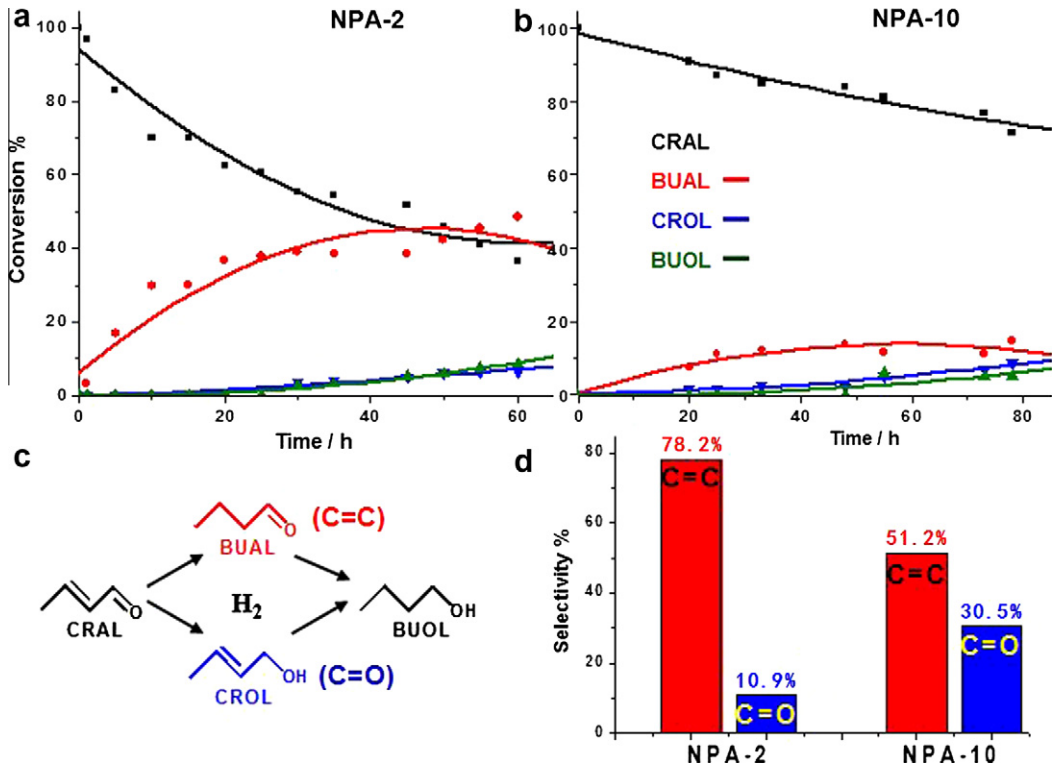

Fig. 6. Time dependent profiles of CRAL hydrogenation over **NPA-2** (a) and **NPA-10** (b) as catalysts, the hydrogenation scheme of CRAL (c) and the selectivity comparison (d).

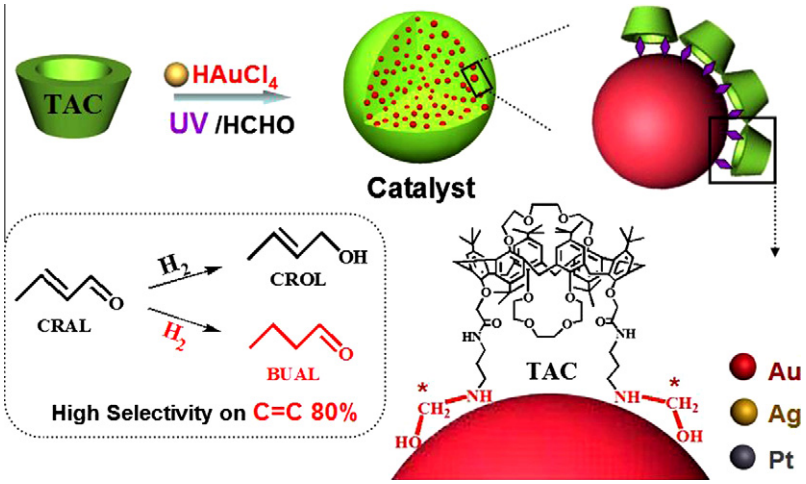

Scheme 2. The Schematic representation of the formation of the **NPA** structures under UV irradiation and the high selectivity of C=C bond using **NPA-2**.

[9], **NPA**s made in this work achieved a higher selectivity to BUAL, which can be explained by that the smaller size of AuNPs is associated with more corners and edges and then lead to a higher catalytic activity [22]. For the control experiment, **NPA-10** gave a much lower selectivity to C=C bond and a lower total conversion, showing an obvious advantage of using smaller AuNPs in **NPA**s (Fig. 6b and Table S2). In addition, no obvious red-shift in the UV spectrum after the catalytic reaction was observed, which indicated no agglomeration of the **NPA**s in the reaction. This was confirmed by the TEM observation (Fig. S6).

4. Conclusion

In summary, hybrid supra-structures were formed from calix[6]biscrown and chloroauric acid. Reduction of $AuCl_4^-$ into AuNPs and the self-assembly of the calixarene happened simultaneously. Under the aid of UV light and formaldehyde, uniform AuNPs with 2 nm diameter were obtained in situ in the organic spheres made of calixarene in a diameter of above 60 nm as shown in Scheme 2. Nanoparticles of Ag and Pt were also prepared following the same procedure, which provide a new Synchronous One-Pot (**SOP**) method to generate self-assembled structures containing metal nanoparticles. Besides, highly chemoselective hydrogenation of crotonaldehyde over the resultant **NPA-2** as catalyst was observed.

Acknowledgments

National Natural Science Foundation China (Nos. 20834004 and 20904005) and Ministry of Science and Technology of China

(2009CB930402 and 2011CB932503) are acknowledged for their financial support. We also thank Prof. Minghua Qiao and Dr. Yan Pei from Department of Chemistry, Fudan University, for their help for the catalytic reaction.

Appendix A. Supplementary material

Supplementary data associated with this article can be found, in the online version, at http://dx.doi.org/10.1016/j.jcis.2012.06.006.

References

[1] (a) Y. Xia, Y. Xiong, B. Lim, S.E. Akrabalak, Angew. Chem., Int. Ed. 48 (2009) 60;
(b) C. Li, K.L. Shuford, Q.H. Park, W. Cai, Y. Li, E.J. Lee, S.O. Cho, Angew. Chem., Int. Ed. 46 (2007) 3264;
(c) R. Costi, A.E. Saunders, U. Banin, Angew. Chem., Int. Ed. 49 (2010) 4878;
(d) M.R. Jones, K.D. Osberg, R.J. Macfarlane, M.R. Langille, C.A. Mirkin, Chem. Rev. 111 (2011) 3736;
(e) T. Mallat, A. Baiker, Chem. Rev. 104 (2004) 3037;
(f) E. Hutter, J.H. Fendler, Adv. Mater. 16 (2004) 1685;
(g) M. Valden, X. Lai, D.W. Goodman, Science 281 (1998) 1647;
(h) G. Budroni, A. Corma, Angew. Chem., Int. Ed. 45 (2006) 3328;
(i) F. Boccuzzi, A. Chiorino, M. Manzoli, P. Lu, T. Akita, S. Ichikawa, M. Haruta, J. Catal. 202 (2001) 256;
(j) K. An, S. Alayoglu, T. Ewers, G.A. Somorjai, J. Colloid Interface Sci. 373 (2012) 1;
(k) J. Zhou, J. Ralston, R. Sedev, D.A. Beattie, J. Colloid Interface Sci. 331 (2009) 251.
[2] (a) M. Grzelczak, J. Vermant, E.M. Furst, L.M. Liz-Marzan, ACS Nano 4 (2010) 3591;
(b) Y. Ofir, B. Samanta, V.M. Rotello, Chem. Soc. Rev. 37 (2008) 1814;
(c) E.R. Zubarev, J. Xu, A. Sayyad, J.D. Gibson, J. Am. Chem. Soc. 128 (2006) 15098;
(d) Y. Lee, H. Lee, P.B. Messersmith, T.G. Park, Macromol. Rapid Commun. 31 (2010) 2109;
(e) J. Song, L. Cheng, A. Liu, J. Yin, M. Kuang, H. Duan, J. Am. Chem. Soc. 133 (2011) 10760;
(f) X. Zhou, Y. Wang, Q. Zhang, et al., Sci. China, Ser. B 41 (2011) 956;
(g) Y. Mai, A. Eisenberg, J. Am. Chem. Soc. 132 (2010) 10078;
(h) E.D. Sone, E.R. Zubarev, S.I. Stupp, Small 2 (2005) 694.
[3] (a) Y. Liu, X. Wang, Polym. Chem. 2 (2011) 2741;
(b) J. Guan, H. Deng, W. Wang, P. Ren, Prog. Chem. 16 (2004) 327.
[4] (a) W. Huang, J.N. Kuhn, C.K. Tsung, Y. Zhang, S.E. Habas, P. Yang, G.A. Somorjai, Nano Lett. 8 (2008) 2027;
(b) R.M. Crooks, M. Zhao, L. Sun, V. Chechik, L.K. Yeung, Acc. Chem. Res. 34 (2001) 181.
[5] (a) Y. Lu, Y. Mei, R. Walker, M. Ballauff, M. Drechsler, Polymer 47 (2006) 4985;
(b) Y. Lu, Y. Mei, M. Drechsler, M. Ballauff, Angew. Chem., Int. Ed. 45 (2006) 813;
(c) Y. Lu, M. Drechsler, Langmuir 25 (2009) 13100;
(d) S. Zhao, M. Cao, L. Li, W. Xu, Acta Chim. Sin. 69 (2011) 492.
[6] (a) C. Song, G. Zhao, P. Zhang, N.L. Rosi, J. Am. Chem. Soc. 132 (2010) 14033;
(b) C.L. Chen, P. Zhang, N.L. Rosi, J. Am. Chem. Soc. 130 (2008) 13555.
[7] B. Guan, M. Jiang, et al., Soft Matter 4 (2008) 1393.
[8] (a) A. Ikeda, S. Shinkai, Chem. Rev. 97 (1997) 1713;
(b) A. Wei, Chem. Commun. (2006) 1581;
(c) R. Balasubramanian, Y.G. Kwon, A. Wei, J. Mater. Chem. 17 (2007) 105;
(d) B. Gadenne, I. Yildiz, M. Amelia, F. Ciesa, A. Secchi, A. Arduini, A. Credi, F.M. Raymo, J. Mater. Chem. 18 (2008) 2022;
(e) Y. Sun, C.G. Yan, Y. Yao, Y. Han, M. Shen, Adv. Funct. Mater. 18 (2008) 3981;
(f) B. Zhao, H. Zhang, Y. Liu, Chin. J. Org. Chem. 8 (2005) 913;
(g) J. Han, C.G. Yan, Prog. Chem. 18 (2006) 1668;
(h) Q. Liang, B. Guan, M. Jiang, Prog. Chem. 22 (2010) 388.
[9] B. Guan, Q. Liang, M. Jiang, et al., J. Mater. Chem. 19 (2009) 7610.
[10] (a) J. Kim, S. Cha, K. Shin, J.Y. Jho, J.C. Lee, Adv. Mater. 16 (2004) 459;
(b) C. Yu, K. Yang, Y. Liu, B. Chen, Mater. Res. Bull. 45 (2010) 838;
(c) K. Chia, R.E. Cohen, M.F. Rubner, Chem. Mater. 20 (2008) 6756.
[11] Q.Y. Yang, Y. Zhu, L. Tian, S.H. Xie, Y. Pei, H. Li, H.X. Li, M.H. Qiao, K.N. Fan, Appl. Catal., A 369 (2009) 67.
[12] K.H. Kim, J.U. Kim, S.H. Cha, J.C. Lee, et al., J. Am. Chem. Soc. 131 (2009) 7482.
[13] (a) A.S.K. Hashmi, G.J. Hutchings, Angew. Chem., Int. Ed. 45 (2006) 7896;
(b) L. He, L.C. Wang, H. Sun, J. Ni, Y. Cao, H.Y. He, K.N. Fan, Angew. Chem., Int. Ed. 48 (2009) 9538.
[14] S. Tan, M. Erol, A. Attygalle, H. Du, S. Sukhishvili, Langmuir 23 (2007) 9836.
[15] Q. Liang, G. Chen, B. Guan, M. Jiang, J. Mater. Chem. 21 (2011) 13262.
[16] K.K. Chia, R.E. Cohen, M.F. Rubner, Chem. Mater. 20 (2008) 6756.
[17] J. Sun, D. Ma, H. Zhang, X. Liu, X. Han, X. Bao, G. Weinberg, N. Pfander, D. Su, J. Am. Chem. Soc. 128 (2006) 15756.
[18] S. Tan, M. Erol, A. Attygalle, H. Du, S. Sukhishvili, Langmuir 23 (2007) 9836.
[19] J. Yang, E.H. Sargent, S.O. Kelley, J.Y. Ying, Nat. Mater. 8 (2009) 683.
[20] (a) E. Bailie, G.J. Hutchings, Chem. Commun. (1999) 2151;
(b) J.E. Bailie, H.A. Abdullah, J.A. Anderson, C.H. Rochester, N.V. Richardson, N. Hodge, J.G. Zhang, A. Burrows, C.J. Kiely, G. Hutchings, J. Phys. Chem. Chem. Phys. 3 (2001) 4113.
[21] M.A. Vannice, B. Sen, J. Catal. 115 (1989) 65.
[22] (a) J. Han, Y. Liu, R. Guo, J. Am. Chem. Soc. 131 (2009) 2060;
(b) H. Tsunoyama, T. Tsukuda, J. Am. Chem. Soc. 127 (2005) 9374;
(c) P. Claus, Appl. Catal., A 192 (2005) 222;
(d) Y. Zhu, L. Tian, Z. Jiang, Y. Pei, S. Xie, M. Qiao, J. Catal. 281 (2011) 106.